Three hTIM mutants that provide new insights on why TIM is a dimer

Mainfroid, Véronique; Terpstra, Peter; Beauregard, Marc; Frère, Jean-Marie; Mande, Shekhar C.; Hol, Wim G.J.; Martial, Joseph A.; Goraj, Karine

Published in:
Journal of Molecular Biology

DOI:
10.1006/jmbi.1996.0174,

Publication date:
1996

J. Mol. Biol. (1996) **257**, 441–456

JMB

Three hTIM Mutants that Provide New Insights on why TIM is a Dimer

Véronique Mainfroid[1], Peter Terpstra[2], Marc Beauregard[3] Jean-Marie Frère[4], Shekhar C. Mande[5], Wim G. J. Hol[5,6] Joseph A. Martial[1]* and Karine Goraj[1]

[1]*Laboratoire de Biologie Moléculaire et de Génie Génétique, Université de Liége, Institut de Chimie, B6 Sart Tilman B-4000, Belgium*

[2]*Department of Chemistry University of Groningen Nijenborgh 16, 9747 Groningen, The Netherlands*

[3]*Chemistry Department University of Prince Edward Island, Charlottetown, PEI C1A4P3, Canada*

[4]*Laboratoire d'Enzymologie Université de Liège, Institut de Chimie, B6, Sart Tilman B-4000, Belgium*

[5]*Department of Biological Structure and the Biomolecular Structure Center, University of Washington, Box 357742 Seattle, WA 98195-7742 USA*

[6]*Howard Hughes Medical Institute, University of Washington, Box 357742 Seattle, WA 98195-7742 USA*

**Corresponding author*

Human triosephosphate isomerase (hTIM), a dimeric enzyme, was altered by site-directed mutagenesis in order to determine whether it can be dissociated into monomers. Two hTIM mutants were produced, in which a glutamine residue was substituted for either Met14 or Arg98, both of which are interface residues. These substitutions strongly interfere with TIM subunit association, since these mutant TIMs appear to exist as compact monomers in dynamic equilibrium with dimers. In kinetic studies, the M14Q mutant exhibits significant catalytic activity, while the R98Q enzyme is inactive. The M14Q enzyme is nevertheless much less active than unmutated hTIM. Moreover, its specific activity is concentration dependent, suggesting a dissociation process in which the monomers are inactive. In order to determine the conformational stability of the wild-type and mutant hTIMs, unfolding of all three enzymes was monitored by circular dichroism and tryptophan fluorescence spectroscopy. In each case, protein stability is concentration dependent, and the unfolding reaction is compatible with a two-state model involving the native dimer and unfolded monomers. The conformational stability of hTIM, as estimated according to this model, is 19.3($\pm$0.4) kcal/mol. The M14Q and R98Q replacements significantly reduce enzyme stability, since the free energies of unfolding are 13.8 and 13.5($\pm$0.3) kcal/mol respectively, for the mutants. A third mutant, in which the M14Q and R98Q replacements are cumulated, behaves like a monomer. The stability of this mutant is not concentration-dependent, and the unfolding reaction is assigned to a transition from a folded monomer to an unfolded monomer. The conformational stability of this double mutant is estimated at 2.5($\pm$0.1) kcal/mol. All these data combined suggest that TIM monomers are thermodynamically unstable. This might explain why TIM occurs only as a dimer.

Keywords: ($\beta\alpha$)-barrel; dimer; protein structure; stability; triosephosphate isomerase

Introduction

Over the past few years, oligomeric proteins have become a major research focus for the information they may yield on quaternary structure formation (Jaenicke, 1987; Jones & Thornton, 1995). Most studies aim to determine whether such proteins can be dissociated into monomers and to probe the properties of isolated monomers. Since the dimer is the least complicated oligomeric structure, mutagenesis experiments have been carried out on a variety of dimeric proteins (Jones *et al*., 1985; Lee *et al*., 1987; Casal *et al*., 1987; Mossing & Sauer, 1990; Borchert *et al*., 1993a,b; Nordoff *et al*., 1993).

Little is known about the properties of single

Abbreviations used: hTIM, human triosephosphate isomerase; CD, circular dichroism; GAP, D-glyceraldehyde-3-phosphate; GDH, glycerol-3-phosphate dehydrogenase.

0022–2836/96/120441–166 $18.00/0

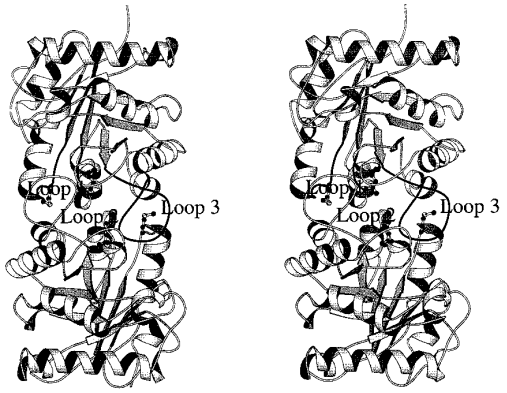

Figure 1. Stereo view of the C^{α} backbone of the hTIM dimer. The β-strands are represented by arrows and the α-helices by spirals. The interface between the two subunits of hTIM is mainly composed of loops 1, 2 and 3. The side-chain of Met14, at the tip of loop 1, and Arg98 are represented.

monomers in the native state of an oligomeric enzyme, since it is often difficult to isolate such monomers without denaturing the protein. One possible strategy is site-directed mutagenesis. By mutating residues at the interface between subunits of an oligomeric protein, one can hope to disrupt the interactions between monomers and destabilize the quaternary structure of the protein. The target of the present study is dimeric triosephosphate isomerase (TIM), which has been well-characterized structurally (Banner *et al*., 1975; Lolis *et al*., 1990; Brändén, 1991; Wierenga *et al*., 1992) and kinetically (Knowles, 1991; Komives *et al*., 1991; Lodi *et al*., 1994).

TIM is the glycolytic enzyme which catalyzes the interconversion of D-glyceraldehyde-3-phosphate and dihydroxyacetone phosphate (Rieder & Rose, 1959). Crystal structures of chicken TIM (Banner *et al*., 1975; Alber *et al*., 1981), yeast TIM (Lolis *et al*., 1990), trypanosomal TIM (Wierenga *et al*., 1991), *Escherichia coli* TIM (Noble *et al*., 1993), human TIM (hTIM, Mande *et al*., 1994) and *Bacillus stearothermophilus* TIM (Delboni *et al*., 1996) have been determined. The TIM subunit has a very regular structure, consisting of an eightfold repeat of a loop–β-strand–loop–α-helix (βα) unit. The eight parallel β-strands form an internal β-barrel surrounded by the eight α-helices (Farber & Petsko, 1990; Goraj *et al*., 1990; Brändén, 1991). The β-strands are numbered β1 to β8 and the α-helices α1 to α8. The eight loops following the β-strands are functionally important and will be referred to as loops 1 to 8. The enzyme is composed of two identical subunits, consisting of 248 residues in the case of the human enzyme. These subunits associate through non-covalent interactions to form a 54 kDa homodimer. Each monomer contains a complete active site, located near the subunit interface but which does not interact directly with the other monomer. TIM, however, is active only as a dimer (Waley, 1973), suggesting that residues of one subunit are crucial for maintaining the integrity of the active site of the other subunit (Wierenga *et al*., 1992).

The extensive interface between the TIM monomers is close to both active sites of the dimer. It is composed essentially of four loops of each monomer (loop 1 to loop 4, Figure 1). Two contacts make a major contribution to the domain

Table 1. Environment of Met14 and Arg98 in hTIM

A. *Interactions of Met14*

(1) Intrasubunit interactions: none

(2) Intersubunit interactions

				d (Å)
Met14	S^{δ}	Tyr367	C^{β}	3.8
Met14	C^{ϵ}	Tyr367	$C^{\delta 2}$	3.6
Met14	C^{ϵ}	Val369	$C^{\gamma 2}$	3.3
Met14	O	Asn371	C^{α}	3.4
Met14	N	Gly372	O	2.8
Met14	C^{α}	Gly372	O	3.4
Met14	O	Gly372	N	2.8
Met14	C^{β}	Gly372	O	3.3
Met14	C^{ϵ}	Gly372	N	3.7
Met14	C^{ϵ}	Phe374	$C^{\delta 2}$	3.3
Met14	S^{δ}	Glu377	C	4.0
Met14	S^{δ}	Glu377	C^{β}	3.7
Met14	S^{δ}	Ile378	N	3.9
Met14	S^{δ}	Ile378	C	3.5
Met14	S^{δ}	Ile378	O	3.3
Met14	S^{δ}	Ser379	N	3.8
Met14	S^{δ}	Ser379	C^{β}	3.8
Met14	C	Met382	C^{ϵ}	3.6
Met14	C^{γ}	Met382	C^{ϵ}	3.7

B. *Interactions of Arg98*

(1) Intrasubunit interactions

				d (Å)
Arg98	N	His95	O	2.8
Arg98	C^{α}	His95	O	3.4
Arg98	C^{β}	His95	O	3.1
Arg98	C^{γ}	His95	O	3.4
Arg98	N	Ser96	C	3.2
Arg98	N	Ser96	O	3.3
Arg98	C	His100	N	3.2
Arg98	O	His100	N	3.2
Arg98	C^{α}	Phe102	C^{β}	3.8
Arg98	C	Phe102	N	3.6
Arg98	O	Phe102	N	2.9
Arg98	O	Phe102	C^{α}	3.1
Arg98	O	Phe102	C	2.9
Arg98	O	Phe102	C^{β}	3.3
Arg98	C^{ζ}	Phe102	C^{γ}	3.7
Arg98	C^{ζ}	Phe102	$C^{\delta 2}$	3.3
Arg98	C^{ζ}	Phe102	$C^{\epsilon 2}$	3.8
Arg98	$N^{\eta 2}$	Phe102	C^{γ}	3.7
Arg98	$N^{\eta 2}$	Phe102	$C^{\delta 2}$	2.9
Arg98	$N^{\eta 2}$	Phe102	$C^{\epsilon 2}$	3.0
Arg98	O	Gly103	N	3.0
Arg98	C	Glu104	N	3.7
Arg98	O	Glu104	N	3.0
Arg98	C^{β}	Glu104	C^{δ}	3.5
Arg98	C^{β}	Glu104	$O^{\epsilon 2}$	3.4

(2) Intersubunit interactions

				d (Å)
Arg98	C^{δ}	Thr375	O	3.0
Arg98	C^{ζ}	Thr375	O	3.4
Arg98	$N^{\eta 2}$	Thr375	C	3.7
Arg98	$N^{\eta 2}$	Thr375	O	2.6
Arg98	$N^{\eta 2}$	Glu377	$O^{\epsilon 1}$	2.9
Arg98	$N^{\eta 2}$	Glu377	$C^{\epsilon 2}$	3.5

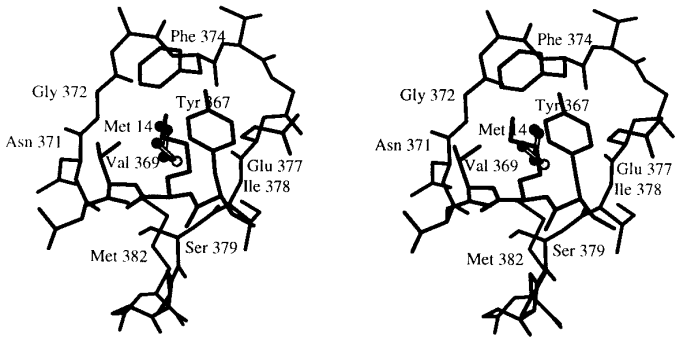

Figure 2. Stereo view of the local environment of Met14 in hTIM. The side-chain of Met14 is encircled by residues from the interface loop of the other subunit (residues 369 to 379). Residues are numbered from 1 to 248 for subunit 1 and from 301 to 548 for subunit 2.

interactions. Most of the intersubunit contacts are mediated by loop 3 (residues 65 to 79, hTIM numbering), also referred to as the interface loop, extending from one subunit into a cavity near the catalytic center of the second subunit. Some residues of this loop interact through van der Waals contacts with the active-site residues of the other subunit (Lolis *et al*., 1990; Wierenga *et al*., 1991, 1992). The tip of loop 3 (residues 74 to 77) forms a hydrophobic pocket around residue 14 of the adjacent subunit. At position 14, hTIM has a methionine, whose side-chain interacts with nine residues of the other subunit (Table 1 and Figure 2). Thus, replacement of Met14 in hTIM is expected to lower the dimer stability, since this residue contributes greatly to the interactions between monomers.

The hydrophobic pockets generated by the interface loop of each monomer account for most of the intersubunit contacts. They lie on the edges of the interface. Between them, there is a polar cavity in which a number of main-chain and side-chain hydrogen bonds, salt bridges, and solvent molecules participate in the subunit interactions. This interface area is centered around residue Arg98, which is surrounded by the side-chains of Phe102, Glu104 and Glu377 (residues are numbered from 1 to 248 for subunit 1 and from 301 to 548 for subunit 2). Glu104 participates in a salt bridge with Lys112, while the guanidinium group of Arg98 is engaged in an interaction with the π system of the phenyl ring of Phe102 (Table 1 and Figure 3). The guanidinium group is also interacting with the main-chain of Thr375 and forms a salt bridge with Glu377 of the other subunit. All these interactions are strictly conserved, suggesting that this part of the interface is important for dimerization and/or enzyme activity. It thus seems plausible that the loss of the Arg98-mediated intersubunit interactions should induce dimer dissociation.

In the present work, we used hTIM as a target for mutagenesis in an attempt to define more precisely the intersubunit contacts that are crucial for maintaining a stable, folded dimer. Our aim was to determine whether the enzyme can be dissociated into stable monomers and to probe the characteristics of the isolated monomers. The initial targets for mutation were residues Met14 and Arg98, whose replacements were expected to perturb the intersubunit interactions stabilizing the dimer conformation.

Results

Production of the M14Q, R98Q, and M14Q/R98Q mutants

Three hTIM mutants were engineered, in which Met14, Arg98, or both were changed to Gln. Expression of the mutated cDNAs was performed in *E. coli* BL21 (DE3) cells, using the T7 system (Studier & Moffatt, 1986). For the single mutants, referred to as M14Q and R98Q, the bacterial culture was grown at 37°C, and both mutants were produced in soluble form, as described for recombinant wild-type hTIM (Mande *et al*., 1994). When the expression of the double mutant, named M14Q/R98Q, was performed at 37°C, the protein accumulated in the bacterial cytoplasm as insoluble inclusion bodies. Production of this mutant was therefore performed at 28°C, since growing the bacterial culture at a lower temperature can favor

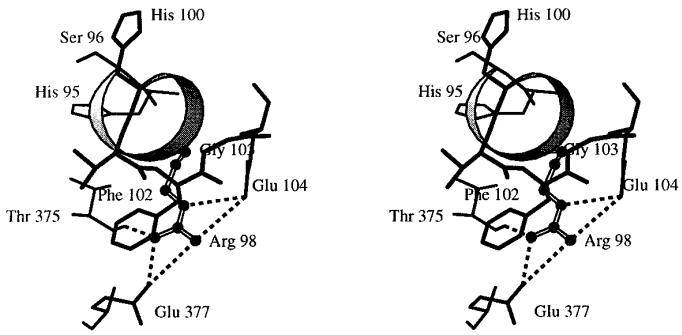

Figure 3. Stereo view of the interactions between Arg98 and its neighbor residues. A linear salt bridge is observed between Glu377, Arg98 and Glu104. Arg98 also interacts with Phe102 and Thr375, while Glu104 participates in a salt bridge with Lys112.

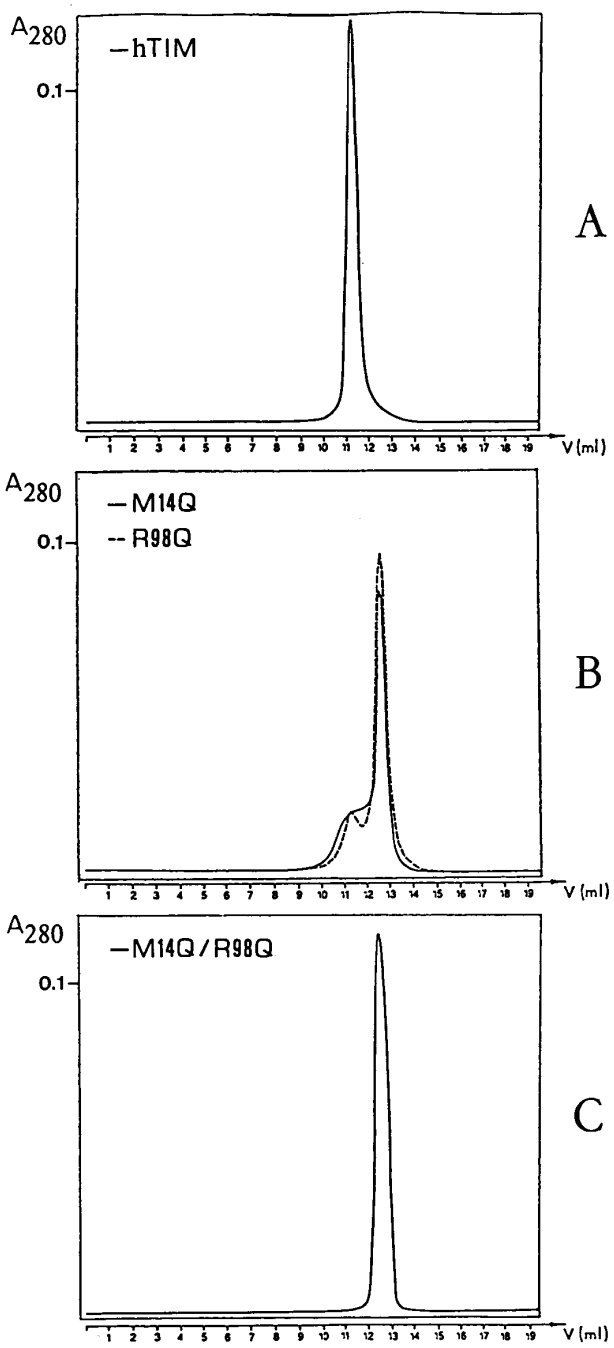

Figure 4. Molecular sieve chromatography of hTIM, M14Q, R98Q, and M14Q/R98Q. A Superose 12 HR 10/30 column was equilibrated in 50 mM Tris-acetate (pH 8), 100 mM NaCl. The flow rate was 0.2 ml/min and the temperature 25°C. A total of 100 μg of each protein in a final volume of 200 μl was loaded onto the column. The elution volume (*V*) is indicated below the profiles. A, hTIM; B, straight lines (M14Q); broken lines (R98Q); C, M14Q/R98Q.

production of a soluble protein (Schein, 1989). Under these conditions, the double mutant was soluble.

The three mutants M14Q, R98Q, and M14Q/R98Q were purified to homogeneity as described (Mande *et al*., 1994). As assessed by denaturing gel electrophoresis, production of the R98Q mutant enzyme equalled that of the corresponding wild-type (100 mg protein/liter of bacterial culture), while mutants M14Q and M14Q/R98Q exhibited 50% reduced production levels. The yield of the purification procedure for all three mutants was similar to that of wild-type hTIM.

Estimated relative molecular masses of the M14Q, R98Q, and M14Q/R98Q mutants

Gel filtration was performed in order to determine association state of the mutant TIMs. On a molecular sieve, wild-type hTIM eluted as a symmetric peak (Figure 4A). The corresponding relative molecular mass, deduced from the elution volumes of standard proteins, was 54,000 ± 1000, in keeping with the enzyme's known dimeric structure. The M14Q and R98Q mutants behaved differently. Gel filtration revealed the presence of two polypeptide forms, a major and a minor one, whose respective relative molecular masses were 28,000 ± 1000 and 54,000 ± 2500 (Figure 4B). Since the theoretical molecular mass of a hTIM monomer is 27 kDa, we concluded that both mutants exist as mixed populations of dimers and compact monomers. At the protein concentration used in the gel filtration experiments (0.5 mg/ml), the dimeric form constitutes only a small fraction of the total protein species population. The M14Q/R98Q mutant behaved like a monomer (Figure 4C) with a relative molecular mass of 28,000 ± 1000.

Activity measurements

In steady-state kinetic measurements, we monitored the specific activity of the mutant enzymes M14Q, R98Q, and M14Q/R98Q at various enzyme concentrations. The TIM assay was initiated by diluting the enzyme in a solution containing the substrate (GAP) and the coupled enzyme system (GDH/NADH).

The specific activity of the M14Q mutant was found to decrease with time, especially at the beginning of the assay. Figure 5 shows this time effect for M14Q (final concentration: 0.5 μg/ml; sample diluted 1000-fold): after 15 minutes, less than 2% of the initial specific activity remains. When different initial protein concentrations were used, it was necessary to leave an interval of at least 15 minutes between dilution and measurement for an equilibrium to be reached. The final activity value was dependent on the initial sample concentration. These findings suggest a time-dependent inactivation of the M14Q mutant upon dilution. They prompted us to incubate all M14Q samples for 20 minutes at 25°C before measuring their activity.

The reversibility of this time-dependent inactivation upon dilution was tested. A 35 μg/ml M14Q solution, with a specific activity of 10.3(±0.2) U/mg, was diluted fivefold to a final concentration of 7 μg/ml. One part of this diluted sample was

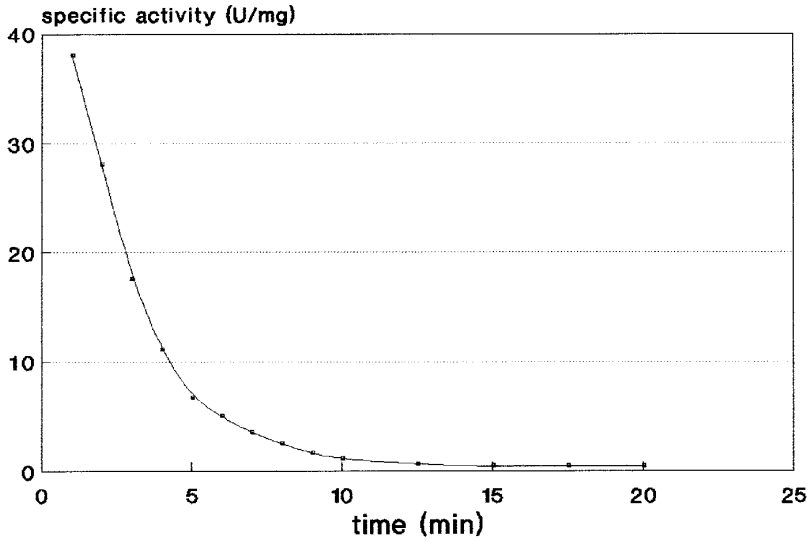

Figure 5. Dilution-dependent inactivation of M14Q. The standard TIM activity assay was initiated by diluting 1 µl of a 0.5 mg / ml protein solution in 1 ml of reaction mixture containing the substrate (GAP) and the coupled enzyme system (GDH-NADH) in 100 mM triethanolamine-HCl (pH 7.6). The remaining specific activity was measured as a function of time.

incubated for 20 minutes at 25°C and its activity assayed, while the other part was reconcentrated (Centricon 10, Amicon CO, MA, USA) to the initial concentration of 35 µg / ml. Its specific activity was then measured at equilibrium. The diluted sample exhibited a specific activity of 4.1($\pm$0.1) U / mg, in keeping with the above observation that dilution causes a large reduction in the specific activity. The specific activity of the reconcentrated sample was 10.1($\pm$0.2) U / m g, which is almost identical to that of the initial sample. This shows that the dilution-dependent inactivation of M14Q is a reversible process.

To determine which form(s) of the M14Q mutant is (are) active, we allowed different dilutions of the M14Q enzyme to equilibrate for 20 minutes at 25°C, then measured the remaining enzyme activity. As shown in Figure 6, the specific activity of the mutant enzyme is highly concentration-dependent at protein concentrations ranging from 10 to 350 10^{-9} M. The shape of the activity *versus* concentration curve is consistent with a protein association reaction, namely a monomer-dimer equilibrium where the monomer is catalytically inactive. We therefore postulate that the activity of the M14Q mutant is due solely to the dimeric form of the enzyme. The same experiment was performed with wild-type hTIM. A dilution-dependent inactivation, similar to that observed for M14Q, was obtained with hTIM at concentrations ranging from 10 to 200 10^{-12} M (Figure 7).

In order to determine the maximum specific activity of M14Q, a theoretical model was constructed, assuming that the TIM dimer is the only active species. This model can be described by:

$$D_{NAT} \overset{K_{DISS}}{\longleftrightarrow} 2M_{NAT} \quad (1)$$

where D_{NAT} is the active dimer, M_{NAT} the inactive monomer and K_{DISS} the dissociation constant.

$$K_{DISS} = [M_{NAT}]^2 / [D_{NAT}] \quad (2)$$

$$[M_{NAT}] = E_o - 2[D_{NAT}] \quad (3)$$

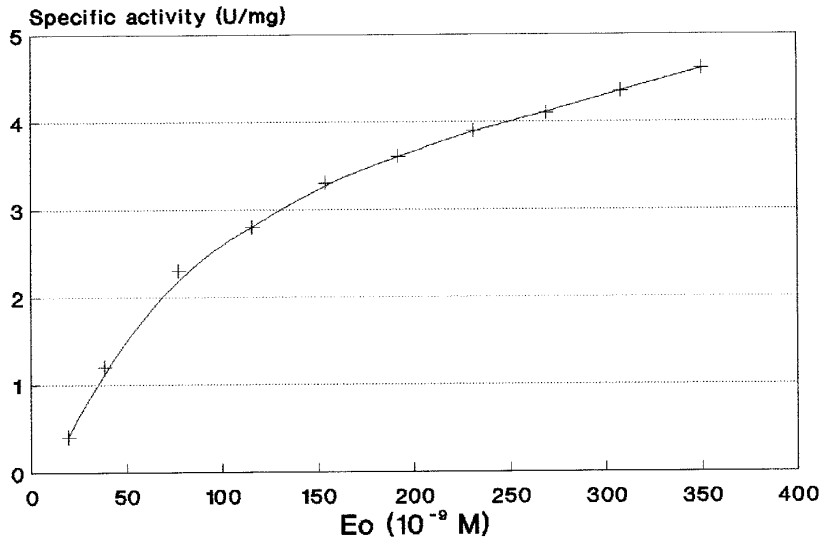

Figure 6. Monitoring of M14Q dimer dissociation by kinetic measurements. The specific activity of M14Q was measured as a function of the protein concentration. To allow the diluted samples to reach equilibrium, we incubated them all for 20 minutes at 25°C prior to performing the measurements.

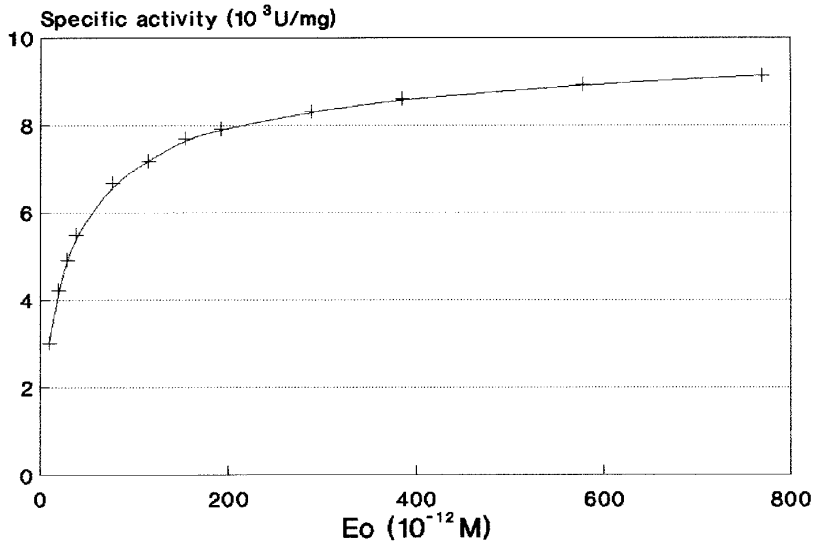

Figure 7. Monitoring of hTIM dimer dissociation by kinetic measurements. The specific activity of wild-type hTIM was measured at different protein concentrations. The diluted samples were incubated for 20 minutes at 25°C to allow equilibrium to be reached.

where E_o is the total monomer concentration when dissociation is complete.

$$SpA = 2SpA_{max}[D_{NAT}]/E_o \quad (4)$$

where SpA is the specific activity and SpA_{max} the maximum specific activity. Therefore:

$$SpA = SpA_{max}[4E_o + K_{DISS} - (8E_oK_{DISS} + K_{DISS}^2)^{1/2}]/4E_o \quad (5)$$

The data from Figures 6 and 7 were fitted to this equation using the EnzFitter program (Leatherbarrow, 1987). For hTIM, K_{DISS} was 32.1($\pm$2.3) 10^{-12} M and SpA_{max} was 10,350($\pm$140) U/mg. For M14Q, we obtained a K_{DISS} value of 45.2($\pm$8.8) 10^{-8} M and a SpA_{max} value of 10.1($\pm$0.1) U/mg, which corresponds to a k_{cat} value of 272 min^{-1}.

To determine the catalytic efficiency of M14Q, the kinetic parameter K_m for this mutant was measured, using a protein concentration of 0.5 µg/ml. It clearly appeared that the K_m value of hTIM is affected by the M14Q replacement (Table 2). The efficiency constant (k_{cat}/K_m) is thus 5200-fold lower for M14Q than for wild-type hTIM. K_i, the inhibition constant determined for the transition state analog 2-phosphoglycolate (Wolfenden, 1969), was also greatly affected, with a value tenfold higher than that of wild-type hTIM (Table 2).

The R98Q and M14Q/R98Q mutants were catalytically inactive at all concentrations tested (0.5 to 100 µg/ml).

Table 2. Kinetic parameters of M14Q

	M14Q	hTIM
K_m (GAP) (mM)	2.56	0.49
k_{cat} (GAP) (min^{-1})	272	2.7 10^5
k_{cat}/K_m (GAP) (min^{-1} mM^{-1})	106	5.5 10^5
K_i (2-phosphoglycolate) (µM)	80	7.4

The values for wild-type hTIM are also indicated.

Spectroscopic studies

Equilibrium denaturation experiments were performed on hTIM and its three mutants to determine the conformational stability of all four proteins. Two spectroscopic methods were used to monitor the denaturation reaction of hTIM and its mutants: the tryptophan fluorescence intensity, and the circular dichroism signal in the far UV. For the experiments monitored by tryptophan fluorescence spectroscopy, both temperature and urea were used as denaturants while for the experiments monitored by CD spectroscopy, only urea was used.

Reversibility of the denaturation process

Thermal unfolding analyses. The reversibility of thermal denaturation was tested on hTIM and its three mutants. A sample of each protein was heated, then cooled to room temperature, and the fluorescence emission spectrum was compared with that of an untreated sample. The recovery of the specific activity of the refolded samples was also checked. Thermal denaturation of hTIM, M14Q, and R98Q was reversible under our conditions. That of the double mutant M14Q/R98Q was not. The results of thermal denaturation are thus only presented for hTIM, M14Q and R98Q.

Urea-induced unfolding analyses. The reversibility of urea denaturation was tested on hTIM and its three mutants. Protein samples were denatured in 8 M urea for 24 hours, then dialyzed against 50 mM Tris-acetate buffer (pH 8). The fluorescence emission and far-UV CD spectra of the dialyzed samples were recorded and compared with those of untreated samples. The good agreement between these spectra indicated that urea denaturation of hTIM and its three mutants is reversible. It took 24 hours for the proteins to fully recover their

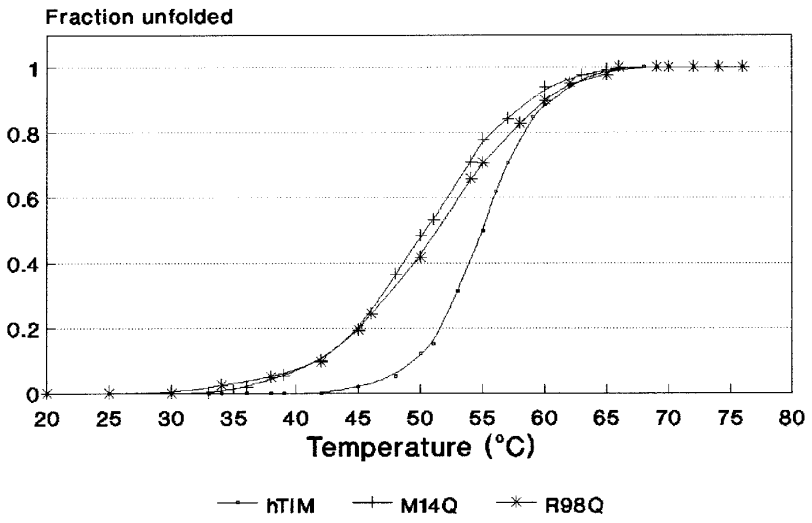

Figure 8. Thermal unfolding curves of hTIM, M14Q, and R98Q obtained from fluorescence measurements. The fraction of unfolded protein at each temperature was calculated from the shift of the fluorescence emission peak following excitation at 290 nm, after correcting for the pre- and post-transition baselines. The data were obtained with 10 μg/ml samples.

spectroscopic characteristics and biological activity (in the case of hTIM and M14Q).

Denaturation of hTIM, M14Q and R98Q

Thermal denaturation monitored by fluorescence. The tryptophan fluorescence emission spectrum for wild-type hTIM recorded at 20°C has its maximum at 323 nm, suggesting that the fluorophores are located in a hydrophobic environment (Burstein, 1976). Thermal denaturation of hTIM resulted in a large decrease in the intrinsic fluorescence intensity, due to thermal quenching (Gally & Edelman, 1964), with a red-shift of the emission peak to 344 nm. This observation is consistent with the transfer of tryptophan residues from a low-polarity medium in native hTIM to the aqueous solvent upon denaturation. The fluorescence emission curves for the M14Q and R98Q mutants are similar. Both native proteins exhibit a peak near 332 nm, suggesting that at least some of the tryptophan residues are more exposed to the solvent than in the native wild-type enzyme. After unfolding, the mutants exhibit the same peak as wild-type hTIM, which suggests that all three enzymes have a similar denatured state.

The shift in the fluorescence emission peak was used to monitor the unfolding reaction. In Figure 8, a plot of the fluorescence emission peak wavelength (λ_{max}) *versus* the temperature for wild-type hTIM reveals a monophasic, sigmoidal curve, indicating a cooperative unfolding transition. Similar plots for the M14Q and R98Q mutants reveal a broader transition between the native state (N) and the denatured state (U). This points to lesser cooperativity during the unfolding process.

To clearly delimit the pre- and post-transition regions in the thermal denaturation curves of TIM and its two single mutants, we used another representation of the data, the so-called ''fluorescent phase plots'' (Burstein, 1977). Figure 9 shows the plots constructed for hTIM and its two mutants using the fluorescence intensities measured at 320

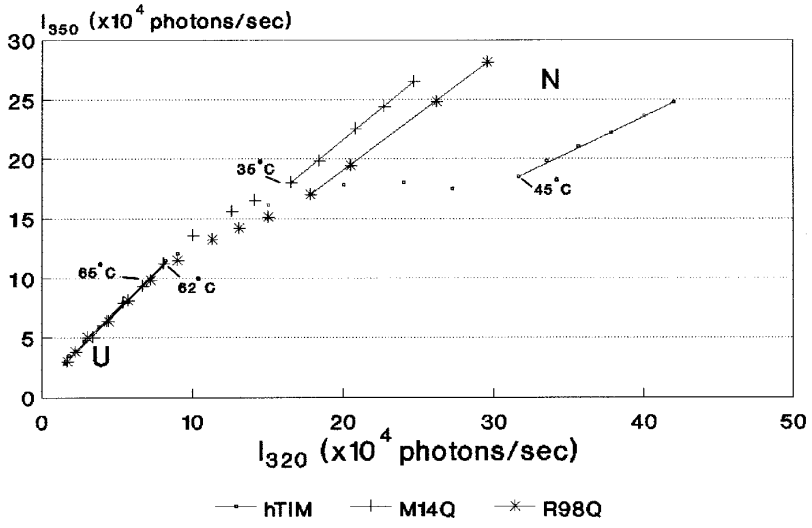

Figure 9. ''Fluorescent phase plots'' obtained from thermal denaturation for hTIM, M14Q, and R98Q, monitored by fluorescence. The fluorescence intensity at 350 nm of the emission spectra recorded at the various temperatures is plotted against the fluorescence intensity at 320 nm. Each point corresponds to a given temperature; 10 μg/ml samples were used. The pre- and post-transition regions are visualized as straight lines, converging at the origin. The native state (N) of each protein corresponds to the lines in the upper part of the graph (low temperatures); the denatured state (U) of each protein is represented by the lines near the origin (high temperatures). The curves connecting N and U correspond to the transition zone.

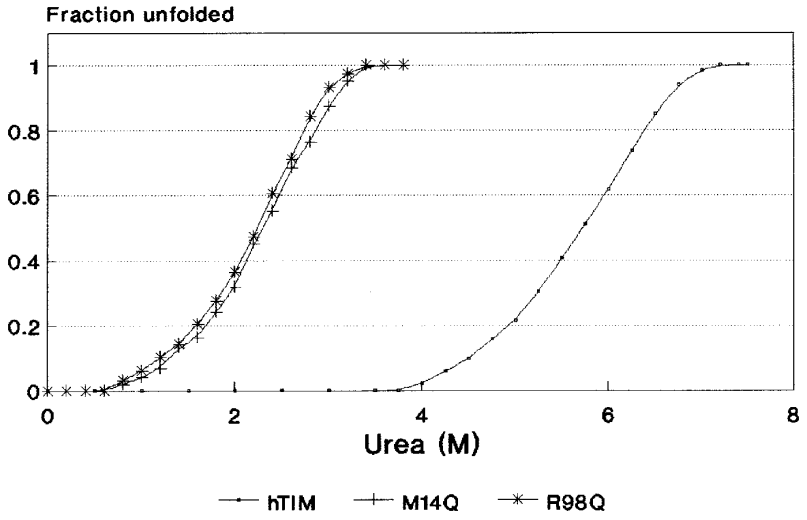

Figure 10. Urea-induced unfolding curves of hTIM, M14Q and R98Q monitored by CD spectroscopy. The fraction of unfolded protein at each urea concentration was calculated from the CD signal at 222 nm after correction for the pre- and post-transition baselines. The data were obtained with 250 μg/ml samples.

and 350 nm (I_{320} and I_{350}) as independent parameters. The three curves describing the ratio of exposed to buried tryptophan identify conformational states in the three proteins. The effect of heating on the native state (N) results in the straight lines in the upper part of the graph, while the denatured state (U) gives rise to the lines near the origin. By means of these fluorescent phase plots, we determined that the transition occurs between 45 and 62°C for hTIM, and between 35 and 65°C for both mutants.

A comparison of the slopes of the straight lines corresponding to the native and unfolded states of the mutant TIMs with those of the wild-type enzyme provided further information. The plots suggest that denatured states of the mutant and wild-type hTIMs are similar. The native wild-type protein state, however, differs significantly from that of the mutants, in agreement with our fluorescence emission measurements.

Urea-induced denaturation monitored by fluorescence. Urea-induced denaturation curves were constructed for hTIM and its two mutants, using the shift in fluorescence emission peak as a variable parameter. A plot of the unfolded fraction *versus* the denaturant concentration revealed a cooperative transition, similar to that observed with thermal denaturation (data not shown). In all three cases, denaturation resulted in a red-shifted emission peak and a twofold increase in the relative fluorescence intensity.

Urea-induced denaturation monitored by CD. CD spectroscopy in the far-UV was used to monitor the urea-induced unfolding of hTIM and its mutants M14Q and R98Q. Upon denaturation, the negative CD signal decreased significantly for all three proteins. Denaturation curves were constructed by following CD changes at 222 nm. In Figure 10, these curves revealed a sigmoidal, monophasic transition from N to U for all three proteins.

Analysis of the denaturation curves of hTIM, M14Q and R98Q. At the concentrations used in the denaturation experiments, hTIM mainly exists as a dimer. The dimeric form of the single mutants is also present in their native state, as determined by molecular sieve chromatography. Thus, the denaturation reaction must start with the folded dimer and end with the unfolded monomer.

The overall equilibrium denaturation reaction of a dimeric protein can be described by two different models, depending on the monomeric states that are present at equilibrium. If the folded monomers are significantly populated in the denaturation transition zone, denaturation can be described by:

$$D_{NAT} \overset{K_1}{\leftrightarrow} 2M_{NAT} \overset{K_2}{\leftrightarrow} 2M_{UNF} \qquad (6)$$

where D_{NAT} is the native dimer, M_{NAT} the folded monomer and M_{UNF} the unfolded monomer.

$$K_1 = [M_{NAT}]^2 / [D_{NAT}]$$

$$K_2 = [M_{UNF}] / [M_{NAT}]$$

Evidence for such a three-state model comes from two observations: a biphasic behaviour of denaturation curves measured by a single probe, and/or the non-coincidence of denaturation curves measured by probes that are sensitive to different levels of protein structure. Such behaviours were observed neither for hTIM, nor for the mutants since in all three cases the unfolding transitions measured by fluorescence or CD spectroscopy were coincident and monophasic.

If the folded monomer (M_{NAT}) is essentially unpopulated at equilibrium, denaturation can be described by a concerted transition from a folded dimer to two unfolded monomers:

$$D_{NAT} \overset{K_D}{\leftrightarrow} 2M_{UNF} \qquad (7)$$

where D_{NAT} is the native dimer and M_{UNF} the unfolded monomer. The equilibrium constant for

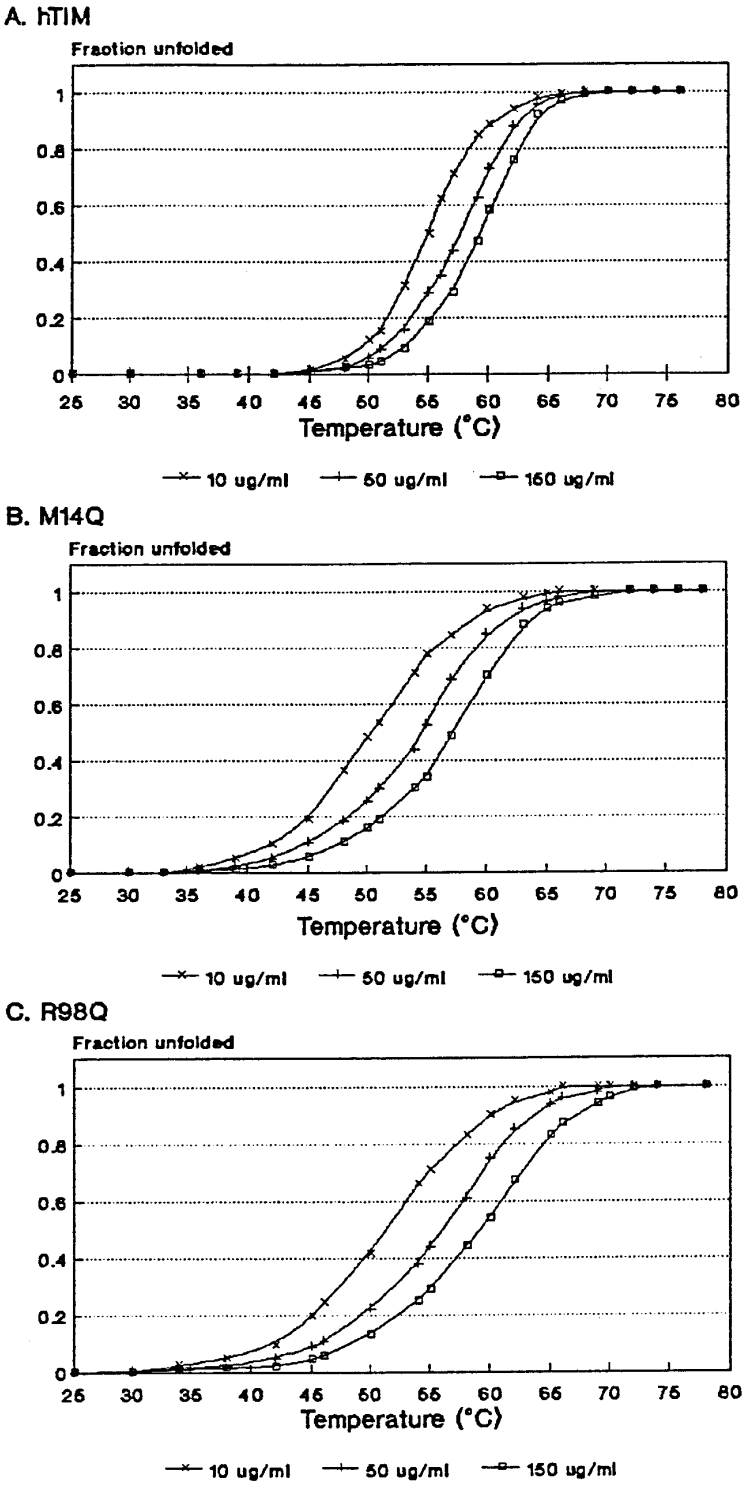

Figure 11. Concentration dependence of thermal denaturation of hTIM (A), M14Q (B) and R98Q (C), monitored by fluorescence spectroscopy. The fraction of protein unfolded at each temperature was calculated at three protein concentrations: x, 10 μg / ml; + , 50 μg / ml; □, 150 μg / ml.

the concerted dissociation-unfolding reaction is given by:

$$K_D = [M_{UNF}]^2 / [D_{NAT}] = 2P_t[\, f_d^2 / (1 - f_d)] \qquad (8)$$

where P_t is the total concentration of protein and f_d the fraction of unfolded protein obtained from the denaturation curves. In thermal denaturation experiments, ΔG_T at temperature T equals:

$$\Delta G_T = \Delta H_1 - (T / T_1)(\Delta H_1 - \Delta G_1) + \Delta C_p[T - T_1 - T \ln(T / T_1)] \qquad (9)$$

where ΔH_1 and ΔG_1 are the enthalpy and free energy of unfolding at temperature T_1, and ΔC_p the heat capacity change for unfolding. In urea-induced denaturation experiments, ΔG equals:

$$\Delta G = -RT \ln K_D \qquad (10)$$

Table 3. Free energies of unfolding for hTIM and its M14Q and R98Q mutants obtained from thermal unfolding experiments monitored by fluorescence

	ΔG_D (kcal / mol)	$\Delta\Delta G_D$ (kcal / mol)
hTIM	19.3 ± 0.4	
M14Q	13.8 ± 0.3	− 5.5
R98Q	13.5 ± 0.3	− 5.8

ΔG_D is the free energy of unfolding at 25°C. $\Delta\Delta G$ is the change in free energy of unfolding of the mutant protein relative to the corresponding wild-type hTIM. A negative value of $\Delta\Delta G$ indicates that the mutant is less stable than the wild-type. The standard deviations are those given by the Enzfitter program (Leatherbarrow, 1987).

If the denaturation of hTIM, M14Q and R98Q can be described by this two-state model, two observations should be made. First, according to the law of mass action, increasing the protein concentration should increase the proportion of native dimer at every denaturant concentration, and the midpoint of the denaturation curves should be shifted to higher denaturant concentrations. To verify this assumption, we constructed fluorescence and CD denaturation curves for hTIM and both mutants over a 15-fold protein concentration range. In all cases, denaturation was found to be concentration-dependent. Figure 11 shows this concentration dependence effect for hTIM, M14Q and R98Q, when thermal denaturation of each protein was monitored by fluorescence. This suggests a dissociation process, and supports the two-state model of denaturation. Second, the validity of the model can be tested by comparing K_D and ΔG_D values calculated at different protein concentrations. If the two-state model provides a good description of the denaturation reaction of all three proteins, one should calculate the same values of K_D and ΔG_D from experiments performed at different protein concentrations. The conformational stabilities of hTIM and its two mutants, calculated from fluorescence and CD experiments performed at different protein concentrations, were the same to within experimental error (data not shown). This further supports the choice of the two-state model of denaturation.

This model was used to analyze the denaturation curves of hTIM, M14Q, and R98Q and to determine their conformational stability at 25°C (ΔG_D). The conformational stability values for hTIM and its mutants calculated from fluorescence experiments are presented in Table 3, while the values obtained from CD measurements are shown in Table 4. The mutants are substantially destabilized as compared to wild-type hTIM.

Denaturation of M14Q/R98Q

Denaturation of the M14Q / R98Q mutant was only performed using urea, since thermal denaturation was found irreversible. Urea-induced denaturation was monitored by fluorescence and CD spectroscopy. Figure 12 shows the urea-induced denaturation curve of M14Q / R98Q monitored by CD.

The protein concentration did not affect the equilibrium of urea denaturation in the case of M14Q / R98Q. The two-state model involving the native dimer and unfolded monomer is therefore unsuitable here, and the folding mechanism of M14Q / R98Q was analyzed by means of a model where only folded and unfolded monomers were present in significant proportion at equilibrium.

This model can be described by:

$$M_{NAT} \leftrightarrow M_{UNF} \qquad (11)$$

where M_{NAT} is the native monomer and M_{UNF} the unfolded monomer. The equilibrium constant, K_D, and the free energy of unfolding, ΔG_D, are given by

$$K_D = f_d / (1 - f_d) \qquad (12)$$

where f_d is the fraction of the protein present in the denatured state.

$$\Delta G_D = -RT \ln(K_D) \qquad (13)$$

The conformational stability of M14Q / R98Q, calculated according to this model, is 2.5(± 0.1) kcal / mol.

Estimation of ΔG_D by accessible surface area calculations

We have estimated the free energy of association of the two TIM monomers in the wild-type hTIM

Table 4. Free energies of unfolding for hTIM, M14Q and R98Q, and M14Q / R98Q calculated from urea-unfolding curves monitored by circular dichroism

	ΔG_D (kcal / mol)	$\Delta\Delta G_D$ (kcal / mol)	m (kcal / mol per M)
hTIM[a]	19.3 ± 0.4		1.7 ± 0.1
M14Q[a]	13.7 ± 0.6	–5.6	2.04 ± 0.15
R98Q[a]	13.5 ± 0.4	–5.8	2.09 ± 0.1
M14Q / R98Q[b]	2.5 ± 0.1		2.65 ± 0.1

ΔG_D is the conformational stability in the absence of urea and m is a measure of the dependence of ΔG on urea concentration. The standards deviations are those given by the EnzFitter program (Leatherbarrow, 1987).

[a] The values presented were obtained using a two-state model of denaturation from folded dimers to unfolded monomers.

[b] The values presented were determined by use of a model involving folded monomers and unfolded monomers (see the text).

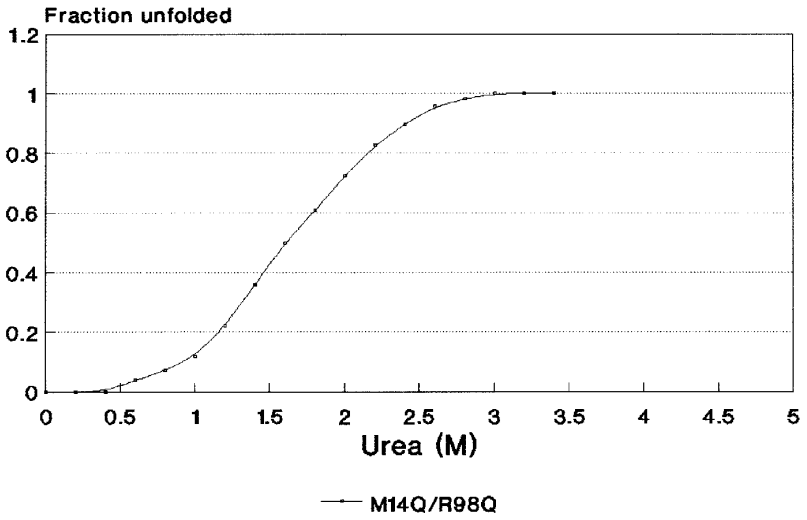

Figure 12. Urea-induced unfolding curve of M14Q/R98Q monitored by CD. The fraction of unfolded protein at each urea concentration was calculated from the CD signal at 222 nm after correction for the pre- and post-transition baselines. The data were obtained with 250 μg/ml samples.

dimer by accessible surface area calculations, on the basis of the crystal structure of hTIM (Mande *et al*., 1994). The free energy of association can be considered as that arising from the unfavorable desolvation of the polar atoms, the favorable desolvation of the non-polar atoms and the loss in entropy of the two individual monomers to form the dimer. Thus:

$$\Delta G_{\text{association}} = \alpha\Delta G_{\text{polar}} + \beta\Delta G_{\text{apolar}} + 2 \times \Delta G_{\text{rotation, translation}}$$

We estimated the fractional accessibilities of individual atoms in the two monomers using the program SURFACE as implemented in the CCP4 (1994) suite. The area buried upon dimerization was considered as the difference between the sum of the areas of the two monomers and that of the dimer. Using these calculations, the area of atoms buried upon dimerization is: 3329.9 Å^2 for carbon, 443.2 Å^2 for nitrogen, 812.9 Å^2 for oxygen, 184.4 Å^2 for sulfur atoms.

Using the Eisenberg and McLachlan parameters for atomic solvations (Eisenberg & McLachlan, 1986), values of 1.4 and 1.2 were obtained for the α and β constants, respectively (Horton & Lewis, 1992). Considering an average of 9 of the suggested 7 to 11 kcal/mol values for the loss in entropy due to fixing one subunit relative to another (Erickson, 1989), we arrived at a value of 14 kcal/mol for $\Delta G_{\text{association}}$ for the wild-type hTIM dimer.

Discussion

We have used site-directed mutagenesis to alter the hTIM dimer interface so as to identify intersubunit contacts which are crucial to dimer formation and stability. Three hTIM mutants were produced by substituting glutamine for Met14, Arg98, or both, and the influence of these changes was examined with regard to quaternary structure formation, enzyme activity, and protein stability.

We have found both the M14Q and R98Q mutants to exist as mixed populations of dimers and monomers, the latter form being predominant under our experimental conditions. This unusual monomer-dimer equilibrium is apparently very similar in both single mutants, since they exhibit the same proportion of monomeric and dimeric forms. Structural considerations may explain the failure of the M14Q and R98Q mutations to completely dissociate the TIM dimer. As compared to that of other dimeric proteins, the subunit interface of TIM is rather large, and the quaternary structure is stabilized by very strong interactions between monomers. This suggests that many intersubunit contacts are crucial for maintaining a stable dimeric structure. Previous studies have identified residues 14 and 98 at two such specific contacts (Wierenga *et al*., 1987, 1991). We show, however, that despite the involvement of these residues in stabilizing interactions, replacing one of them is not enough to cause complete dissociation of the TIM dimer. This suggests that it might be possible to produce a completely monomeric, non-dimerizing mutant by altering more than one intersubunit contact residue. To check this assumption, we engineered a double mutant cumulating both the M14Q and R98Q replacements. Since this M14Q/R98Q mutant is completely monomeric, it would appear that changing two contact residues, which greatly contribute to subunit interactions, is sufficient to completely shift the dimer-monomer equilibrium towards the monomeric form.

The two single mutations have very different effects on enzyme activity. The R98Q mutant is inactive and although its crystallographic structure is not yet available, analysis of the wild-type hTIM structure may provide some explanation. Arg98 lies near the subunit interface in a pocket dominated by the charged side-chains of Glu104, Lys112, and Glu377. Buried charged amino acids are not found frequently in proteins, and buried salt bridges tend to be conserved across a family of protein structures. TIMs are no exception, and all these residues are well conserved in the known TIM sequences. Replacement of Arg98 would lead to the disruption of two salt bridges, Arg98–Glu377 and

Arg98–Glu104; this would affect the delicate balance of partial charges and might thereby destabilize loop 3. Moreover, since Arg98 is in contact with the catalytic His95, replacement of Arg98 by Gln might affect this interaction, thereby preventing the correct positioning of His95 in the active site, and rendering the mutant enzyme inactive.

The M14Q mutant retains significant enzyme activity, so we wondered to which form, the monomer or the dimer, this activity might be attributed. Isolated monomers of oligomeric proteins are frequently inactive (Jaenicke, 1987), although monomers of aldolase (Chan & Mawer, 1972; Chan *et al*., 1973a) and yeast *trans*-aldolase (Chan *et al*., 1973b) have been shown to possess catalytic activity. The specific activity of the M14Q mutant is concentration-dependent, which strongly suggests that dissociation could be responsible for the loss of activity. We therefore postulate that the TIM dimer is the only active species in the M14Q mutant, and that quaternary interactions are required for M14Q enzyme activity. This is in keeping with the findings of Waley (1973), who suggested that individual TIM subunits are catalytically inactive. A similar dilution-dependent inactivation process has been reported by Borchert *et al*. (1993a) for a mutated trypanosomal TIM in which His47 was replaced with Asn, further supporting the hypothesis that TIM monomers are inactive. A monomeric TIM mutant, exhibiting significant catalytic activity, was, however, reported by Borchert *et al*. (1993b). This protein, named monoTIM, was engineered by replacing the interface loop in trypanosomal TIM (tTIM) with an eight-residue fragment. Analysis of the crystal structure of monoTIM revealed that modifying loop 3 in tTIM leads to further structural rearrangements, since some interface loops, mainly loops 1 and 4, had adopted new structural properties. Interestingly, loop 1 contains the catalytic Lys13, while loop 4 contains the catalytic His95. It was shown that the orientation of these two residues was drastically modified, as compared to their location in wild-type tTIM. It is highly probable that the unexpected catalytic activity of monoTIM is due to these particular rearrangements. Such modifications are not expected in our M14Q/R98Q hTIM monomer.

The M14Q/R98Q TIM monomer was inactive. This lack of activity is, however, not surprising, since one of the parental mutants, R98Q, is already inactive.

To determine the conformational stability of hTIM and its three mutants, the denaturation process of all four proteins was monitored by circular dichroism and fluorescence spectroscopy, which are sensitive to different levels of protein structure. Two different models were used to interpret our results. For hTIM, M14Q, and R98Q, the equilibrium between a folded dimer and two unfolded monomers was considered, whereas for the monomeric M14Q/R98Q, the data were analyzed by means of model involving a transition from a folded monomer to an unfolded monomer.

For wild-type hTIM, M14Q and R98Q, the change in free energy upon unfolding, ΔG_D, was determined with a two-state model of denaturation involving the folded dimer and unfolded monomer. Unfolding of homodimeric proteins has been frequently found to be two-state, although monomeric intermediates have been reported in a few cases (Herold & Kirschner, 1990; Eftink *et al*., 1994). The common observation of a two-state folding/unfolding reaction in dimeric proteins presumably applies, since the high denaturant concentrations required to dissociate individual subunits do not allow the monomeric states to be sufficiently stable and folded. Thus, the transiently stable monomeric states get masked in the monophasic denaturation curves. In such cases, the individual monomers can only be observed at low denaturant concentrations (or temperatures) in which they are stable. Achieving a balance for denaturation concentrations sufficient to dissociate the dimers into monomers, and yet observing the very unstable monomers, more or less rules out the denaturation experiments using denaturants or temperature. We therefore believe that unfolding of TIM dimers is a two-step (three-state) process, initially dissociating dimers into minimally stable and compact monomers, and then unfolding the monomers.

The use of a common two-state model of denaturation for hTIM and its M14Q and R98Q mutants suggests that the native and unfolded states are the same in all three proteins. By means of molecular sieve chromatography, we noted that the native state of hTIM is mainly composed of dimers, while that of the mutants is mainly composed of monomers. We should, however, keep in mind that the native state of a dimeric protein always contains a small fraction of its monomeric form, the amount of which depends on the dissociation constant and the sample concentration. The native state of hTIM, M14Q and R98Q is thus composed of a mixture of dimers and monomers, the former being favored in hTIM, while the latter is favored in the mutants. The equilibrium to be considered during unfolding of the three proteins is thus the same, but the use of ''D_{NAT}'' to describe the native state of hTIM, M14Q and R98Q should more likely be replaced by another term, which would take into account the presence of both dimeric and monomeric forms.

The conformational stability of hTIM, as determined by independent methods, was estimated at 19.3 kcal/mol. This is consistent with the values commonly determined for globular proteins, ranging from 5 to 15 kcal/mol (Pace, 1990). An increasing number of dimeric proteins are now being analyzed in stability studies. It appears that the conformational stabilities of such proteins are generally quite high as compared to those of monomeric proteins (Neet & Timm, 1994), and the value obtained for hTIM is in good agreement with these observations. The M14Q and R98Q replacements significantly reduced the stability of the hTIM dimer, and they were found to exhibit about

the same conformational stability, with ΔG_D values of 13.8 (M14Q) and 13.5 (R98Q) kcal / mol.

The conformational stability of the M14Q / R98Q monomeric mutant was calculated using a model of denaturation typical of monomeric proteins, which involves the folded monomer and the unfolded monomer. The free energy of denaturation of this monomeric mutant was estimated at 2.5 kcal / mol, a value lower than those usually obtained for monomeric proteins (Pace, 1990).

In addition to the denaturation experiments which provided ΔG_D values for hTIM and its three mutants, different experiments were achieved to get an estimate of ΔG_{DISS}, the stability of the hTIM dimer relative to the folded monomer. The kinetic data in Figures 6 and 7 allowed the determination of K_{DISS} values for wild-type hTIM and M14Q, which were of 32.1 10^{-12} M and 45.2 10^{-8} M, respectively. The corresponding free energies of dissociation, ΔG^{WT}_{DISS} and ΔG^{M14Q}_{DISS}, are 14.32 kcal / mol and 8.66 kcal / mol, respectively. Using accessible surface area calculations, a theoretical ΔG_{DISS} value of 14 kcal / mol was obtained for wild-type hTIM.

In order to bring all our data together and to interpret our results, theoretical analyses were undertaken. We postulated that the free energy of formation of unfolded monomers from folded dimers, ΔG_D, is composed of the free energy of dimer dissociation, ΔG_{DISS}, and the free energy of monomer unfolding, ΔG_{UNF}, even if M_{NAT} gets masked in some experiments. Thus:

$$D_{NAT} \overset{\Delta G_{DISS}}{\longleftrightarrow} 2M_{NAT} \overset{\Delta G_{UNF}}{\longleftrightarrow} 2M_{UNF} \qquad (14)$$

where D is the dimer and M is the monomer.

$$\Delta G_D = \Delta G_{DISS} + 2\Delta G_{UNF} \qquad (15)$$

For hTIM, ΔG_D was estimated at 19.3 kcal / mol using equilibrium denaturation experiments, and ΔG_{DISS} was estimated at 14.3 kcal / mol through independent experiments: namely (1) concentration-dependent inactivation of the enzyme, (2) urea and temperature dependent unfolding observed by fluorescence, (3) urea-dependent unfolding observed by circular dichroism and (4) theoretical calculation based on atomic solvation parameters. Substituting these values in equation (15), we arrive at:

$$\Delta G_{UNF} = 2.5 \text{ kcal / mol} \qquad (16)$$

The conformational stability of a hTIM monomer is thus very low as compared to that of the hTIM dimer.

The conformational stability of our hTIM monomeric mutant, M14Q / R98Q, was found to be 2.5 kcal / mol, which is in remarkable correlation with the value arrived at above in equation (16). It is thus very attractive to propose that the M14Q and R98Q replacements did not affect the stability, and hence the structure, of the hTIM monomers. For M14Q, this is very likely, since Met14 is fully solvent accessible once the dimer is dissociated, and is only involved in intersubunit interactions. Moreover, the values of ΔG_D (13.8 kcal / mol) and ΔG_{DISS} (8.8 kcal / mol) for the M14Q mutant, obtained from equilibrium denaturation experiments and activity measurements, respectively, also lead to a conformational stability of 2.5 kcal / mol for the M14Q monomers. For the R98Q replacement, the situation could, however, be different, since Arg98 makes intrasubunit contacts with residues from its own subunit. Replacing Arg98 with a glutamine could thus significantly destabilize the hTIM monomers. However, only the end of the side-chain is different in R98Q compared to wild-type enzyme, and hence this substitution is also likely to have only limited effects on monomer conformation and stability. Moreover, the value of ΔG_D for R98Q (13.5 kcal / mol) is close to that of M14Q, suggesting that both mutants must have a similar dissociation constant. This is in agreement with the fact that both single mutants exhibit the same proportion of monomer and dimer at a given protein concentration on a molecular sieve. We therefore propose that the calculations deduced for M14Q also hold for R98Q. Finally, if the R98Q replacement was destabilizing, the conformational stability of the monomeric M14Q / R98Q mutant would be lower than 2.5 kcal / mol, but this was not observed. We thus postulate that the free energy of unfolding associated with the transition from a folded monomer to an unfolded monomer in hTIM was not significantly affected by the M14Q and R98Q replacements.

The low stability of isolated TIM monomers, about 2.5 kcal / mol, may provide indications as to the advantage of quaternary structure formation in the case of the hTIM enzyme. Apart from being necessary for enzyme activity, subunit assembly may also ensure maximal conformational stability. The present results are consistent with this conclusion, since the folded hTIM dimer is essentially stabilized through quaternary interactions which account for 75% of the overall conformational stability of the protein. The folded monomer is only weakly stabilized as compared to the unfolded monomer, so one way for the folded TIM monomer to reach a higher level of stability is by subunit assembly. All these considerations could explain why TIM, in its present form, occurs only as a dimer.

Materials and Methods

Mutagenesis and protein purification

The M14Q and R98Q single mutations were introduced by site-directed mutagenesis (Kunkel, 1985) into wild-type hTIM cDNA (Mande *et al*., 1994) cloned into bacteriophage M13mp19. The mutant primers used were synthetic 21 bp oligonucleotides (Eurogentec, Seraing, Belgium). Both mutations were confirmed by sequencing the altered cDNAs. The mutant cDNAs were subcloned into the expression vector pARHS-3 (De Moerlooze *et al*., 1992), giving rise to vectors pARHS-M14Q and pARHS-R98Q. The expression vector harboring the cDNA encoding the M14Q / R98Q double mutant was constructed by introducing a 75 bp *Nco*I-*Sac*I DNA fragment

of hTIM containing the M14Q mutation into plasmid pARHS-R98Q restricted with the same enzymes.

Protein production and purification were performed as described (Mande *et al*., 1994). The homogeneity of the purified enzymes was assessed by SDS/polyacrylamide gel electrophoresis (Laemmli, 1970).

Apparent molecular mass determination

Molecular sieve chromatography was performed on a Superose 12 HR 10/30 column (Pharmacia, Uppsala, Sweden) eluted at 25°C and at a flow rate of 0.2 ml/min. The buffer used was 50 mM Tris-acetate (pH 8.0) containing 100 mM NaCl. Bovine serum albumin (68 kDa), ovalbumin (45 kDa), prolactin (23 kDa) and myoglobin (17.5 kDa) were used as standards.

Activity measurements

TIM activity was monitored by the decrease in the absorbance at 340 nm due to oxidation of NADH in a coupled-enzyme assay at 25°C. The reaction was carried out according to Misset & Opperdoes (1984) in a 1 ml cuvette containing 100 mM triethanolamine-HCl (pH 7.6) 20 μg/ml glycerol-3-phosphate dehydrogenase, 0.24 mM NADH, 0.12 to 9.95 mM D-glyceraldehyde-3-phosphate, and TIM (concentration as specified) to initiate the reaction. One activity unit (U) corresponds to the conversion of 1 μmol substrate/minute at 25°C under our standard assay conditions. Kinetic parameters were determined as described (Mande *et al*., 1994).

Fluorescence analyses

Tryptophan fluorescence spectroscopy was used to analyze the denaturation of hTIM and of its three mutants, since one hTIM subunit contains five tryptophan residues, located in ($\beta\alpha$)-units 1 (W12), 4 (W90) and 6 (W157, 168 and 191).

Thermal unfolding

Equilibrium fluorescence measurements were carried out on a PTI MS-III spectrofluorometer. For tryptophan fluorescence intensity measurements, the excitation was set at 290 nm and the emission was scanned from 300 to 400 nm with a 4 nm band-pass in both excitation and emission. All spectra were corrected for buffer and water emission and for loss of efficiency in the detector and grating. The sample temperature was controlled with a Lauda R6S circulating bath. The cell temperature was calibrated against the bath temperature with a Parr 1671 precision thermometer. Measurements were performed in a 1 cm quartz cuvette. The protein concentration was 10 μg/ml in 50 mM Tris-acetate buffer (pH 8.0). The samples were incubated for 5 to 20 minutes at each temperature prior to fluorescence measurements. The incubation time was varied as more time was required to reach equilibrium at high temperatures. Thermal unfolding curves were obtained by monitoring the shift of the fluorescence emission peak. Thermodynamic data were obtained by Van't Hoff analysis of the denaturation curves (Brandts, 1964; Pace *et al*., 1989) using the EnzFitter program (Leatherbarrow, 1987). ΔC_p, the heat capacity change for unfolding, was calculated by measuring T_m and ΔH_m as a function of pH, and was estimated at 1.5 kcal/(mol.deg) (Privalov & Khechinashvili, 1974). The buffers used were 50 mM Tris-acetate (pH 8), 50 mM acetate-Tris (pH 4), and 50 mM phosphate (pH 6 and pH 7). The pre- and post-transition regions of the unfolding curves were delimited by means of ''fluorescent phase plots'' (Burstein, 1977).

Urea-induced unfolding

Fluorescence measurements were performed with a Perkin-Elmer LS-50 spectrofluorometer. The samples were excited at 290 nm and the emission recorded from 300 to 400 nm. The bandwidths used in excitation and emission were 7 and 15 nm, respectively. Measurements were performed at 25°C in a 1 cm quartz cuvette. The protein concentration was 10 μg/ml in 50 mM Tris-acetate buffer (pH 8). The spectra were corrected for the background fluorescence of the urea-containing buffer. Equilibrium denaturation was performed by incubating protein samples at each urea concentration for 24 hours at room temperature. Analysis of the denaturation data was performed as described (Pace *et al*., 1989) using the EnzFitter program (Leatherbarrow, 1987).

Circular dichroism (CD)

CD measurements were performed at 25°C on a CD6 dichrograph (SA-Jobin-Yvon, Longiumeau, France) with 0.1 cm path length quartz cuvettes. Sample concentrations of 250 μg/ml in 50 mM Tris-acetate (pH 8), were used. Urea-induced denaturation was monitored by CD changes at 222 nm. Protein samples were incubated for 24 hours at the various urea concentrations prior to CD measurements to reach equilibrium. All values were averaged over five measurements and corrected for the buffer and urea signal.

Acknowledgements

We are grateful to Dr Rik Wierenga for stimulating discussions and critical comments. We thank Dr Marc Vanhove for help with the theoretical calculations in kinetic and spectroscopic analyses. V. M. acknowledges the support of IRSIA fellowships. This work was supported by grants from the EC-BRIDGE program (BIOT-CT90-0182) and from the Services Fédéraux des Affaires Scientifiques, Techniques, et Culturelles–PAI P3-044. M.B. acknowledges the support of a grant from SCRUG-UPEI.

References

Alber, T., Banner, D W., Bloomer, A. C., Petsko, G. A., Phillips, D. C., Rivers, P. S. & Wilson, I. A. (1981). On the three-dimensional structure and catalytic mechanism of triosephosphate isomerase. *Phil. Trans. Roy. Soc. ser. B*, **293**, 159–171.

Banner, D. W., Bloomer A. C., Petsko, G. A., Phillips, D. C., Pogson, C. I., Wilson, I. A., Corran, P. H., Furth, A. J., Milman, J. D., Offord, R. E., Priddle, J. D. & Waley, S. G. (1975). Structure of chicken muscle triosephosphate isomerase determined crystallographically at 2.5 Å resolution using amino acid sequence data. *Nature*, **255**, 609–614.

Borchert, T. V., Pratt, K., Zeelen, J. Ph., Callens, M., Noble, M. E. M., Opperdoes, F. R., Michels, P. A. M. & Wierenga, R. K. (1993a). Overexpression of trypanosomal triosephosphate isomerase in *Escherichia*

coli and characterization of a dimer-interface mutant. *Eur. J. Biochem.* **211**, 703–710.

Borchert, T. V., Abagyan, R., Radha Kishan, K. V., Zeelen, J. Ph. & Wierenga, R. K. (1993b). Structure of an engineered monomeric triosephosphate isomerase, monoTIM: the correct modelling of an eight-residue loop. *Structure*, **1**, 205–213.

Brändén, C. I. (1991). The most frequently occuring folding motif in proteins–the TIM barrel. *Curr. Opin. Struct. Biol.* **1**, 978–983.

Brandts, J. F. (1964). The thermodynamics of protein denaturation. *J. Am. Chem. Soc.* **86**, 4291–4301.

Burstein, E. A. (1976). *Luminescence of Protein Chromophores*. vol. 6, *Model Studies. Science and Technology Results. Biophysics*, VINITI, Moscow.

Burstein, E. A. (1977). *Intrinsic Protein Luminescence*. vol. 7, *Origin and Applications. Science and Technology Results. Biophysics*, VINITI, Moscow.

Casal, J. I., Ahern, T. J., Davenport, R. C., Petsko, G. A. & Klibanov, A. M. (1987). Subunit interface of triosephosphate isomerase: site-directed mutagenesis and characterization of the altered enzyme. *Biochemistry*, **26**, 1258–1264.

CCP4 Suite (1994). Programs for protein crystallography. *Acta Crystallog. sect. D*, **50**, 760–763.

Chan, W. W. C. & Mawer, H. M. (1972). Protein subunits–preparation and properties of active subunits of aldolase bound to a matrix. *Arch. Biochem. Biophys.* **149**, 136–145.

Chan, W. W. C., Mort, J. S., Chong, D. K. K. & Macdonald, P. D. M. (1973a). Protein subunits–kinetic evidence for the presence of active subunits during the renaturation of muscle aldolase. *J. Biol. Chem.* **248**, 2778–2784.

Chan, W. W. C., Schutt, H. & Brand, K. (1973b). Active subunits of transaldolase bound to Sepharose. *Eur. J. Biochem.* **40**, 533–541.

Delboni, L. F., Mande, S. C., Rentier-Delrue, F., Mainfroid, V., Turley, S., Vellieux, F. M. D., Martial, J. A. & Hol, W. G. J. (1995). Crystal structure of recombinant triosephosphate isomerase from *Bacillus stearothermophilus*. An analysis of potential thermostability factors in six isomerases with known three dimensional structures points to the importance of hydrophobic interactions. *Protein Sci.* **4**, 2594–2604.

De Moerlooze, L., Struman, I., Renard, A. & Martial, J. A. (1992). Stabilization of T7-promoter-based pARHS expression vectors using the *parB* locus. *Gene*, **119**, 91–93.

Eftink, M. R., Helton, K. J., Beavers, A. & Ramsay, G. D. (1994). The unfolding of *trp* aporepressor as a function of pH: evidence for an unfolding intermediate. *Biochemistry*, **33**, 10220–10228.

Eisenberg, D. & McLachlan, A. D. (1986). Solvation energy in protein folding and binding. *Nature*, **319**, 199–203.

Erickson, H. P. (1989). Co-operativity in protein-protein association. The structure and stability of the actin filament. *J. Mol. Biol.* **206**, 465–474.

Farber, G. K. & Petsko, G. A. (1990). The evolution of α/β barrel enzymes. *Trends Biochem. Sci.* **15**, 228–234.

Gally, J. A. & Edelman, G. M. (1964). Effects of conformation and environment on the fluorescence of proteins and polypeptides. *Biopolymers, Symp.* **1**, 367–381.

Goraj, K., Renard, A. & Martial, J. A. (1990). Synthesis, purification and initial structural characterization of octarellin, a *de novo* polypeptide modelled on the α/β-barrel proteins. *Protein Eng.* **3**, 259–266.

Herold, M. & Kirschner, K. (1990). Reversible dissociation and unfolding of aspartate aminotransferase from *Escherichia coli*: characterization of a monomeric intermediate. *Biochemistry*, **29**, 1907–1913.

Horton, N. & Lewis, M. (1992). Calculation of the free energy of association for protein complexes. *Protein Sci.* **1**, 169–181.

Jaenicke, R. (1987). Folding and association of proteins. *Prog. Biophys. Mol. Biol.* **49**, 117–237.

Jones, D. H., McMillan, A. J. & Fersht, A. R. (1985). Reversible dissociation of dimeric tyrosyl-tRNA synthetase by mutagenesis at the subunit interface. *Biochemistry*, **24**, 5852–5857.

Jones, S. & Thornton, J. M. (1995). Protein-protein interactions: a review of protein dimer structures. *Prog. Biophys. Mol. Biol.* **63**, 31–65.

Knowles, J. R. (1991). Enzyme catalysis: not different, just better. *Nature*, **350**, 121–124.

Komives, E. A., Chang, L. C., Lolis, E., Tilton, R. F., Petsko, G. A. & Knowles, J. R. (1991). Electrophilic catalysis in triosephosphate isomerase: The role of histidine-gs. *Biochemistry*, **30**, 3011–3019.

Kunkel, T. A. (1985). Rapid and efficient site-specific mutagenesis without phenotypic selection. *Proc. Natl Acad. Sci. USA*, **82**, 488–492.

Laemmli, U. K. (1970). Cleavage of structural proteins during the assembly of the head of the bacteriophage T4. *Nature*, **227**, 680–685.

Leatherbarrow, R. J. (1987). Enzfitter: a non-linear regression data analysis program for the IBMPC/P52. Elsevier Biosoft, Cambridge, UK.

Lee, E. H., Soper, T. S., Mural, R. J., Stringer, C. D. & Hartman, F. C. (1987). An intersubunit interaction at the active site of D-ribulose-1,5-bisphosphate carboxylase/oxygenase as revealed by cross-linking and site-directed mutagenesis. *Biochemistry*, **26**, 4599–4604.

Lodi, P. J., Chang, L. C., Knowles, J. R. & Komives, E. A. (1994). Triosephosphate isomerase requires a positively charged active site: the role of lysine-12. *Biochemistry*, **33**, 2809–2814.

Lolis, E., Alber, T., Davenport, R. C., Rose, D., Hartman, F. C. & Petsko, G. A. (1990). Structure of yeast triosephosphate isomerase at 1.9 Å resolution. *Biochemistry*, **29**, 6609–6618.

Mande, S. C., Mainfroid, V., Kalk, K. H., Goraj, K., Martial, J. A. & Hol, W. G. J. (1994). Crystal structure of recombinant human triosephosphate isomerase at 2.8 Å resolution. *Protein Sci.* **3**, 810–821.

Misset, O. & Opperdoes, F. R. (1984). Simultaneous purification of hexokinase, class-I fructose-bisphosphate aldolase, triosephosphate isomerase and phosphoglycerate kinase from *Trypanosoma brucei*. *Eur. J. Biochem.* **144**, 475–483.

Mossing, M. C. & Sauer, R. T. (1990). Stable, monomeric variants of λcro obtained by insertion of a designed β-hairpin sequence. *Science*, **250**, 1712–1715.

Neet, K. E. & Timm, D. E. (1994). Conformational stability of dimeric proteins: quantitative studies by equilibrium denaturation. *Protein Sci.* **3**, 2167–2174.

Noble, M. E. M., Zeelen, J. P., Wierenga, R. K., Mainfroid, V., Goraj, K., Gohimont, A. C. & Martial, J. A. (1993). Structure of triosephosphate isomerase from *E. coli* determined at 2.6 Å resolution. *Acta Crystallog. sect. D*, **49**, 403–417.

Nordoff, A., Bücheler, U. S., Werner, D. & Schirmer, R. H. (1993). Folding of the four domains and dimerization are impaired by the Gly446-Glu exchange

in human glutathione reductase. Implications for the design of antiparasitic drugs. *Biochemistry*, **32**, 4060–4066.
Pace, C. N. (1990). Conformational stability of globular proteins. *Trends Biochem. Sci.* **15**, 14–17.
Pace, C. N., Shirley, B. A. & Thomson, J. A. (1989). Measuring the conformational stability of a protein. In *Protein Structure: A Practical Approach* (Creighton, T. E., ed.), pp. 311–330, IRL Press, Oxford.
Privalov, P. L. & Khechinashvili, N, N. (1974). A thermodynamic approach to the problem of stabilization of globular protein structure: a calorimetric study. *J. Mol. Biol.* **86**, 665–684.
Rieder, S. V. & Rose, I. A. (1959). The mechanism of the triosephosphate isomerase reaction. *J. Biol. Chem.* **234**, 1007–1010.
Schein, C. H. (1989). Production of soluble recombinant proteins in bacteria. *Biotechnology*, **7**, 1141–1148.
Studier, F. W. & Moffatt, B. A. (1986). Use of bacteriophage T7 RNA polymerase to direct selective high-level expression of cloned genes. *J. Mol. Biol.* **189**, 113–130.
Vriend, G. (1990). WHAT IF: a molecular modeling and drug design program. *J. Mol. Graph.* **8**, 52–56.
Waley, S. G. (1973). Refolding of triosephosphate isomerase. *Biochem. J.* **135**, 165–172.
Wierenga, R. K., Kalk, K. H. & Hol, W. G. J. (1987). Structure determination of the glycosomal triosephosphate isomerase from *Trypanosoma brucei brucei* at 2.4 Å resolution. *J. Mol. Biol.* **198**, 109–121.
Wierenga, R. K., Noble, M. E. M., Vriend, G., Nauche, S. & Hol, W. G. J. (1991). Refined 1.83 Å structure of trypanosomal triosephosphate isomerase crystallized in the presence of 2.4 M ammonium sulphate. A comparison with the structure of the trypanosomal triosephosphate isomerase–glycerol-3-phosphate complex. *J. Mol. Biol.* **220**, 995–1015.
Wierenga, R. K., Noble, M. E. M. & Davenport, R. C. (1992). Comparison of the refined crystal structures of liganded and unliganded chicken, yeast and trypanosomal triosephosphate isomerase. *J. Mol. Biol.* **224**, 1115–1126.
Wolfenden, R. (1969). Transition state analogues for enzyme catalysis. *Nature*, **233**, 704–705.

Edited by A. R. Fersht

(Received 10 January 1995; accepted in revised form 5 January 1996)